Journal of General Virology (2006), **87**, 267–276 DOI 10.1099/vir.0.81476-0

Neuropathogenesis of herpesvirus papio 2 in mice parallels infection with *Cercopithecine herpesvirus 1* (B virus) in humans

Kristin M. Rogers, Jerry W. Ritchey, Mark Payton, Darla H. Black and R. Eberle

Department of Veterinary Pathobiology, Center for Veterinary Health Sciences, Oklahoma State University, 250 McElroy Hall, Stillwater, OK 74078-2007, USA

Correspondence
Kristin M. Rogers
kristin.m.rogers@okstate.edu

Cercopithecine herpesvirus 1 (monkey B virus; BV) produces extremely severe and usually fatal infections when transmitted from macaque monkeys to humans. *Cercopithecine herpesvirus 16* (herpesvirus papio 2; HVP2) is very closely related to BV, yet cases of human HVP2 infection are unknown. However, following intramuscular inoculation of mice, HVP2 rapidly invades the peripheral nervous system and ascends the central nervous system (CNS) resulting in death, very much like human BV infections. In this study, the neurovirulence of HVP2 in mice was further evaluated as a potential model system for human BV infections. HVP2 was consistently neurovirulent when administered by epidermal scarification, intracranial inoculation and an eye splash. Quantitative real-time PCR, histopathology and immunohistochemistry were used to follow the temporal spread of virus following skin scarification and to compare the pathogenesis of neurovirulent and apathogenic isolates of HVP2. Apathogenic isolates were found to be capable of reaching the CNS but were extremely inefficient at replicating within the CNS. It is concluded that neurovirulent strains of HVP2 exhibit a pathogenesis in mice that parallels that observed in human BV infections and that this model system may prove useful in dissecting the viral determinants underlying the extreme severity of zoonotic BV infections.

Received 31 August 2005
Accepted 30 September 2005

INTRODUCTION

Cercopithecine herpesvirus 1 (monkey B virus; BV) is a ubiquitous pathogen of macaques (*Macaca* spp.). In captive animals, BV is most often acquired as an oral infection by infants and juveniles or as a genital infection in sexually mature animals. In many respects the biology of BV is comparable to that of herpes simplex virus (HSV) in humans and *Cercopithecine herpesvirus 16* (herpesvirus papio 2; HVP2) in baboons (*Papio* spp.). While there have been no reported cases of human HVP2 infection, BV is well known for its extreme neuropathogenicity when transmitted to non-macaque primates, including humans (Davidson & Hummeler, 1960; Weigler, 1992; Whitley & Hilliard, 2001). Although zoonotic BV infections are rare, the extreme severity of these infections has resulted in BV being classified as the only biosafety level 4 (BSL-4) herpesvirus. Furthermore, the US Government classifies BV as a 'select agent' due to concern regarding its potential use as a bioterrorism weapon.

Due to the hazardous nature of BV and the requirement for special biocontainment facilities, relatively little research has been done on the virus. An additional difficulty has been the lack of a small animal system which faithfully and reproducibly portrays zoonotic BV infections. Although rabbits are quite sensitive to BV infection, their size and cost and the lack of analytical reagents make this a less than ideal model system. The development of a small animal model that accurately depicts human BV infections will be of use not only in studying zoonotic BV infections but also for investigating the more general question regarding zoonoses: what mechanisms cause some viruses to be so extremely neurovirulent when introduced into a non-natural host species?

Several studies have examined the mouse as a potential small animal model system for studying BV neurovirulence (Gosztonyi *et al.*, 1992; Ritchey *et al.*, 2005). Although very young animals are quite sensitive to BV infection (Gosztonyi *et al.*, 1992), a number of concerns regarding the use of a murine model to study cross-species BV infections have been identified. Firstly, the pathogenicity of different strains of BV in mice varies across the full range of virulence phenotypes from completely apathogenic to extremely neurovirulent (Ritchey *et al.*, 2005). Secondly, the virulence of individual BV isolates in mice is variable depending on the route of inoculation (J. W. Ritchey, D. H. Black and R. Eberle, unpublished data). Finally, BV infections in mice are not strictly dose-dependent, so calculation of infectious and lethal doses can be difficult (Ritchey *et al.*, 2005).

Therefore, while a BV/mouse model may be appropriate for examining certain aspects of BV infections, this system may not be suitable for molecular and genetic analyses aimed at examining the viral mechanisms which determine the outcome of a cross-species BV infection.

In contrast to the wide range of pathogenic phenotypes of BV observed in mice, intramuscular (i.m.) inoculation of mice with multiple isolates of HVP2 revealed quite a different picture in that all isolates tested fell into one of two distinct subtypes, highly neurovirulent (HVP2nv) or apathogenic (HVP2ap) (Rogers *et al.*, 2003). While all HVP2nv isolates tested produced fulminant, fatal, central nervous system (CNS) infections equivalent to those induced by the most pathogenic strains of BV, HVP2ap-inoculated mice never showed clinical signs of infection (Rogers *et al.*, 2003). In addition, despite the very high degree of genetic relatedness between BV and HVP2, HVP2 is a BSL-2 pathogen. Thus, all indications are that an HVP2nv/mouse model system may be a safe, consistent and reproducible model for human BV infections.

Initial experiments with HVP2 in mice used i.m. inoculation to simulate infection via a monkey bite. While a number of human BV infections have resulted from bites, several other routes of transmission have been implicated, including eye splashes, scratches from macaques or contaminated equipment and needle sticks. To validate fully the usefulness of the HVP2nv/mouse system as a model for zoonotic BV infections, it was necessary to assess whether the pathogenic phenotypes observed after i.m. inoculation of mice remained consistent using additional routes of infection. Further, it was important to characterize both the temporal and spatial distribution of HVP2 infection in the mouse CNS. Finally, it was necessary to distinguish between the neuroinvasive and neurovirulent capacity of HVP2ap to determine whether the differences between HVP2nv and HVP2ap were due to the inability of HVP2ap to enter and/or replicate within the CNS.

METHODS

Viruses and cells. Vero cells were cultured in complete Dulbecco's modified Eagle's medium (DMEM) containing 10 % fetal bovine serum (FBS) and maintained in DMEM containing 2 % FBS. The origin of all HVP2 isolates as well as the purification of viral DNA have been described previously (Eberle *et al.*, 1995, 1997, 1998; Rogers *et al.*, 2003).

Mouse inoculations. Female BALB/c mice, weighing 10–12 g (intra-cranial and eye splash inoculation) or 12–14 g (skin scarification) were obtained from Charles River Laboratories. For inoculation, mice were immobilized by anaesthetic inhalation (IsoFlo; Abbott Laboratories). Once infected, mice were observed twice daily for clinical signs of infection. All mice were humanely euthanized by CO_2 inhalation when clinical signs of infection became severe or at the termination of the experiment. Sterile PBS was used as diluent for all viral dilutions and as inoculum for negative-control mice.

For skin scarification (s.s.), groups of eight mice were shaved and an 8 mm circle was drawn on the left rear flank to identify the inoculation site. A 22-gauge needle was used to scarify the skin superficially inside the circle and 10 µl inoculum containing tenfold dilutions of HVP2nv isolate X313 or HVP2ap isolate OU2-5 ranging from 10^2 to 10^6 p.f.u. was applied to the site with a micropipettor.

For eye splash (e.s.) inoculation, 5 µl inoculum containing tenfold dilutions of HVP2nv isolate OU1-76 ranging from 10^1 to 10^6 p.f.u. or HVP2ap isolate OU2-5 ranging from 10^4 to 10^6 p.f.u. was placed directly into the left eye of mice in groups of five using a micropipettor.

For temporal studies, groups of 72 mice were inoculated by s.s. with 10^5 p.f.u. HVP2nv isolate X313, HVP2ap isolate OU2-5 or diluent as described above. Six mice from each group were euthanized daily on days 1–9 post-infection (p.i.). Skin from the inoculation site, sections of lumbar and thoracic spinal cord and brainstem tissue were harvested from three mice in each group and stored at −80 °C. The remaining three mice from each group were processed for histopathological examination.

For intracranial (i.c.) inoculation, groups of five mice were inoculated using a 50 µl syringe (model 705LT; Hamilton) with a 27-gauge needle to deliver 10 µl inoculum containing 10^2–10^6 p.f.u. HVP2ap isolates A951 or OU2-5, 10^0–10^6 p.f.u. HVP2nv isolate X313 or diluent into the cerebrum.

Sample preparation. To obtain template DNA for the real-time PCR assay, total DNA was extracted from tissue samples using the DNAeasy Tissue kit (Qiagen) according to the manufacturer's protocol except that the amount of proteinase K was doubled, DNA was eluted in a 100 µl final volume and 15 µl 0·25 % linear polyacrylamide was added to all spinal cord samples prior to ethanol precipitation of the DNA (Gaillard & Strauss, 1990). DNA samples were dehydrated in an Eppendorf Vacufuge and stored at −20 °C. All DNA samples were resuspended in 10 mM Tris/HCl pH 8·0 (brain and inoculation site epithelial DNA in 200 µl, spinal cord tissue DNA in 35 µl) and quantified by spectroscopy.

Real-time quantitative PCR assay. To avoid potential problems with the real-time assay due to subtype-specific sequence variation, HVP2-specific primers and probe were designed from an alignment of the HVP2 UL41 open reading frame (ORF) sequence of four HVP2ap isolates and four HVP2nv isolates using the PRIMEREXPRESS software (version 2.0; Applied Biosystems). The sequence of the forward primer (5′-TGCGCCAACCTCTACCA-3′) and reverse primer (5′-TGTCGGTCGTGTGGACGT-3′) as well as a TaqMan MGB probe (5′-CCAACACCGTCGCG-3′) labelled at the 5′ end with FAM (6-carboxyfluorescein) and at the 3′ end with a non-fluorescing quencher were all designed from the nucleotide alignment of the eight HVP2 sequences. Primers/probes and all real-time PCR reagents, disposables and equipment were purchased from Applied Biosystems. PCRs were performed in a 96-well plate and contained 1× TaqMan Universal PCR master mix, 2·0 µM each primer, 10 nM probe and 2·0 µl sample DNA in a final volume of 25 µl. The TaqMan pre-designed assay for 18S rRNA was used as directed by the manufacturer. PCR amplification and detection were performed on an ABI Prism 7000 Sequence Detection System using the following cycling conditions: 50 °C for 2 min, 95 °C for 10 min and 40 two-step cycles of 95 °C for 15 s and 60 °C for 1 min. All PCRs were carried out in triplicate with appropriate controls run on each plate.

HVP2 DNA and cellular DNA standards. For use as a viral standard in the PCR assay, an 800 bp segment of the HVP2 UL41 ORF was amplified by standard PCR using the forward primer HVP2-492 (5′-GCATGTTGGAGAAGGCGGAGCTGG-3′) and the reverse primer HVP2-493 (5′-GACTGGTGCGGAGGGGAGGTTGG-3′) (Sigma-Genosys). The Invitrogen TOPO TA cloning kit was used to clone the PCR product and the fidelity of the insert was confirmed by

DNA sequencing. Purified plasmid DNA was isolated using the Qiagen Plasmid maxi kit and quantified by spectroscopy. The plasmid standard was used as described on the Applied Biosystems website (http://www.appliedbiosystems.com/support/tutorials/pdf/quant_pcr.pdf). The dynamic range for detection of the HVP2 plasmid standard by the real-time PCR assay was 10^0–10^5 viral genome copies (VGC) per reaction.

To correlate 18S rRNA C_T values with mouse cell numbers as a means of normalizing for variable tissue mass, two 25 cm^2 flasks of subconfluent mouse L929 cells at different cell densities were counted using a haematocytometer. Suspensions containing $1{\cdot}3 \times 10^6$ and $3{\cdot}1 \times 10^6$ cells were centrifuged at 300 ***g*** for 5 min and each cell pellet was resuspended in 500 µl sterile PBS for DNA extraction. The 18S rRNA assay was used to detect the number of 18S rRNA genes in a tenfold dilution series of the two DNA samples. The 18S C_T values showed a linear decrease with increasing L929 cell DNA over a dynamic range of $<10^0$ to $1{\cdot}3 \times 10^4$ cells. Cellular 18S C_T values were plotted against the number of 18S genes per reaction to generate a standard curve using Microsoft Excel 2003. Regression analysis was used to calculate the number of mouse cells present in unknown DNA samples based on the 18S C_T values.

Correlation between viral genome copies and infectious virus. To validate the use of real-time PCR for quantifying HVP2 in tissue samples, it was necessary to correlate the number of VGC to the number of infectious virions (p.f.u.). Mice in groups of two were inoculated by s.s. with 10^5 p.f.u. HVP2nv isolate OU1-76 or HVP2ap isolate OU2-5. Mice were euthanized at 7 days p.i. and tissue samples were collected from the site of inoculation, spinal cord, brainstem and spleen. After the tissue samples were homogenized in 500 µl DMEM with 2 % FBS (750 µl for inoculation-site skin samples), 450 µl of the liquid was removed, divided equally into two sterile microcentrifuge tubes and placed at −80 °C. The Qiagen QIAamp 96 DNA Blood kit was used to extract total DNA from one aliquot for use as template in quantitative real-time PCR assay. The second aliquot was used to quantify infectious virus using a standard plaque assay (Eberle & Hilliard, 1984).

The minimum detection threshold for the plaque assay was $2{\cdot}0 \times 10^1$ p.f.u. ml^{-1}. Based on validation of the real-time assay using the viral standard, the minimum detection level of VGC was $5{\cdot}0 \times 10^2$ VGC ml^{-1}. Log values of p.f.u. ml^{-1} were plotted against log values of VGC ml^{-1} and the correlation coefficient was calculated using Microsoft Excel 2003 (Fig. 1). The correlation coefficient ($r = 0{\cdot}978$) demonstrates a strong positive correlation between VGC and p.f.u. in all positive tissue samples. Although there were only two HVP2ap-positive samples, the correlation between VGC and p.f.u. for these samples was the same as for HVP2nv-positive samples. Thus, the sensitivity of the real-time assay was similar regardless of HVP2 subtype. On average, for both HVP2nv and HVP2ap, each p.f.u. correlated to approximately 10^4 VGC.

Histopathology and immunoassays. Blood was collected by cardiac puncture at the time of death/euthanasia and the serum was stored at −80 °C until tested by ELISA to detect anti-HVP2 IgG as described previously (Ohsawa *et al.*, 1999; Rogers *et al.*, 2003). All histological procedures were conducted as described previously (Breshears *et al.*, 2001; Ritchey *et al.*, 2002). For mice inoculated i.c., brains were removed at the time of death/euthanasia and submerged in buffered formalin until dissected for histological examination.

Statistical analyses. The 50 % infectious dose (ID_{50}), 50 % clinical disease dose (CD_{50}), 50 % CNS disease dose ($CNSD_{50}$) and 50 % lethal dose (LD_{50}) were calculated by probit regression with PROC PROBIT in PC SAS version 8.2 (SAS Institute). The values calculated were compared by methods developed for effective dosages (Robertson & Preisler, 1992). The ID_{50} was defined by the presence of serum anti-HVP2 IgG in mice that survived to at least 10 days p.i. for s.s. experiments or 7 days p.i. for the i.c. inoculation. Mice that died prior to 10 days p.i. were assumed to be infected and were included as positives for calculation of ID_{50} values. CD_{50} values were calculated based on mice that developed skin lesions while $CNSD_{50}$ values were based on mice that exhibited clinical signs of CNS disease. LD_{50} values were based on animals that either died as a result of the infection or required euthanasia due to the severity of disease.

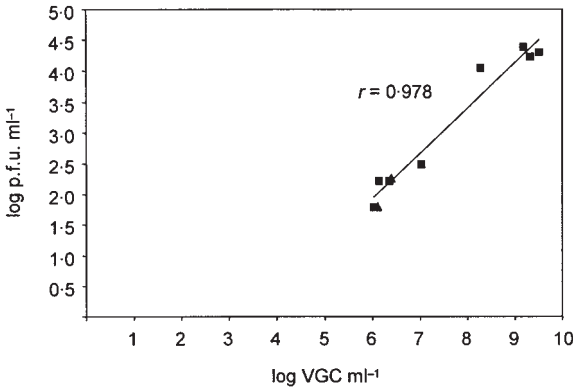

Fig. 1. Correlation of VGC to p.f.u. Tissue samples representing skin, spinal cord, spleen and brainstem from two HVP2nv-infected mice (■) and two HVP2ap-infected mice (▲) were assayed for VGC by real-time PCR and p.f.u. values were determined by plaque assay. Each data point represents the mean VGC ml^{-1} value for triplicate real-time PCRs and p.f.u. ml^{-1} for duplicate plaque assays. Although there were only two HVP2ap-positive samples, the correlation between VGC and p.f.u. for these samples was the same as for HVP2nv-positive samples.

RESULTS

HVP2 pathogenicity via skin scarification

We showed previously that HVP2ap was clinically apathogenic in mice following i.m. inoculation while HVP2nv infection resulted in rapid paralysis and death (Rogers *et al.*, 2003). To determine whether the two mouse-defined pathogenic phenotypes were consistent following a different route of inoculation, mice were inoculated via s.s. with HVP2 at doses ranging from 10^2 to 10^6 p.f.u. All mice inoculated with 10^6 p.f.u. HVP2nv developed lesions at the inoculation site as well as elsewhere within the dermatome by 4–5 days p.i. (Fig. 2a). Mice infected with 10^2–10^5 p.f.u. HVP2nv also developed lesions at the site of inoculation, with some delay in the appearance of the lesions with lower virus doses (Table 1). In contrast, small lesions confined to the site of inoculation were observed 6–7 days p.i. in mice inoculated with 10^5–10^6 p.f.u. of HVP2ap (Fig. 2b). These lesions resolved by 9–10 days p.i.; however, at 12–13 days p.i., a few of these same mice developed new lesions, primarily at or near the site of inoculation, ipsilateral hind limb and/or ipsilateral inguinal region. A single mouse inoculated with 10^4 p.f.u. HVP2ap developed a small lesion at the site of

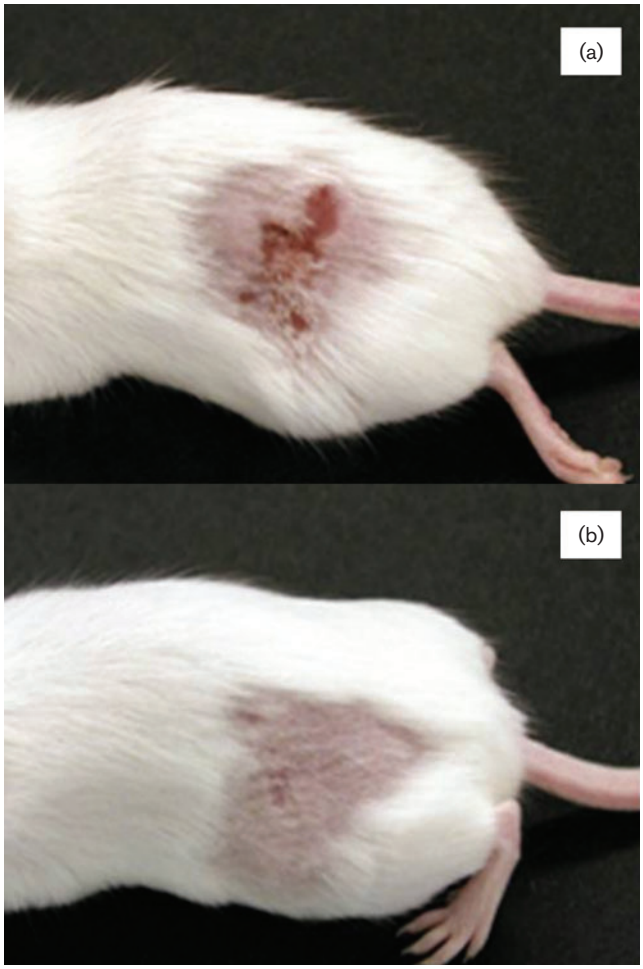

Fig. 2. Skin lesions at 6 days p.i. in mice infected s.s. with 10^6 p.f.u. HVP2. In addition to more severe lesions at the site of inoculation, HVP2nv-infected mice (a) displayed ipsilateral flaccid hind limb paralysis by 6 days p.i., which was not noted in any HVP2ap-infected mice (b) throughout the experiment.

inoculation at 13 days p.i. Mice inoculated with doses lower than 10^4 p.f.u. HVP2ap never showed any clinical signs of disease. Based on these data, the CD_{50} values were determined to be $10^{2\cdot7}$ p.f.u. for HVP2nv and $10^{5\cdot8}$ p.f.u. for HVP2ap.

Based on the presence of serum anti-HVP2 IgG, the ID_{50} value for HVP2ap-infected mice was $10^{3\cdot9}$ p.f.u. (Table 1). All HVP2nv-infected mice inoculated by s.s. that exhibited signs of CNS disease succumbed to the infection, resulting in identical ID_{50}, $CNSD_{50}$ and LD_{50} values of $10^{2\cdot9}$ p.f.u. In contrast, $CNSD_{50}$ and LD_{50} values for HVP2ap by s.s. were $>10^6$ p.f.u., with no HVP2ap-infected mice requiring euthanasia.

Temporal and spatial distribution of HVP2 infection in mice

Mice were inoculated by s.s. with 10^5 p.f.u. HVP2 for several purposes: (i) to determine the time required for HVP2nv to enter the CNS, (ii) to evaluate the anatomical distribution of HVP2 infection within the mouse CNS and (iii) to quantify the spread of HVP2nv compared with HVP2ap. At various time points, skin from the inoculation site, lumbar spinal cord, thoracic spinal cord and brainstem were harvested, DNA was extracted and VGC per cell was quantified by real-time PCR. As shown in Fig. 3(a), DNA from both HVP2 subtypes was detected at all time points from skin at the site of inoculation; however, HVP2nv DNA was present at significantly higher levels than HVP2ap on four of the seven days. HVP2nv was detected in both the lumbar and thoracic regions of the spinal cord by 4 and 5 days p.i., respectively, with the amount of virus in both regions increasing between 5 and 7 days p.i. (Fig. 3b, c). In contrast, HVP2ap DNA was not detected in the spinal cord until 5–6 days p.i. and at significantly lower levels than HVP2nv DNA. Viral DNA was also detected at significant levels in the brainstem of all HVP2nv-infected mice between 6 and 7 days p.i. (Fig. 3d), while HVP2ap was never detected in the brainstem throughout the experiment.

Following s.s. inoculation, detectable histological lesions were restricted to the skin, spinal cord and brainstem. By 3 days p.i., the epidermis of HVP2nv-infected mice exhibited hyperplasia as well as necrosis of epithelial cells, intranuclear inclusion bodies and viral antigen immunoreactivity within epithelial cells of the epidermis and hair follicles (Fig. 4a, b). At 5 days p.i., these lesions had progressed to full-thickness necrosis of the epidermal and follicular epithelium, formation of serocellular crusts and intense infiltrates of neutrophilic and mononuclear inflammatory cells within the dermis and subcutis. Evidence of viral infection within the epithelium of HVP2ap-infected mice was evident by 5 days p.i. and was characterized by occasional scant necrosis of epithelial cells, neutrophilic and mononuclear dermal infiltrate and the formation of surface crusts; however, full-thickness necrosis of the epithelium and herpetic inclusion bodies were not conspicuous. By immunohistochemistry (IHC), positive staining was located mostly within the epidermis and hair follicles in HVP2ap-infected mice (Fig. 4c, d).

Despite the lack of clinical signs of CNS infection in HVP2ap-infected mice, the development of CNS lesions was similar for the two HVP2 subtypes, differing primarily in the severity of tissue destruction and intensity of viral antigen detected by IHC. In HVP2nv-infected mice, lesions characterized by swelling and necrosis of dorsal root ganglion (DRG) cells and a mild infiltration by mononuclear inflammatory cells as well as viral antigen were first detected at 4 days p.i. In HVP2ap-infected mice, a level of involvement comparable to HVP2nv was not seen in the DRG until 6 days p.i. While lesions in the DRG of HVP2nv-infected mice progressed with significant inflammation and loss of ganglion cells, DRG lesions in HVP2ap-infected mice did not progress over time. Further, the intensity of IHC staining was always greater in HVP2nv-infected tissues.

Table 1. HVP2 pathogenesis in mice following s.s. inoculation

Entries for clinical signs are number of mice showing clinical signs/number in group. Mean times of death are shown in parentheses in days p.i. For the ELISA, absorbance shows the mean A_{490} for positive sera (positive cut-off $\geqslant 0{\cdot}100$) for anti-HVP2 IgG in serum from mice collected 10–19 days p.i. Numbers in parentheses are the range of A_{490} values of positive sera. Seropositivity shows the number of positive sera/total number of sera tested. Sera were not tested for mice that died prior to 10 days p.i.; NSA, no sera available for testing.

Dose (p.f.u.)	Clinical signs			ELISA	
	Skin lesions	CNS signs	Death	Absorbance	Seropositivity
HVP2nv					
10^6	7/7	7/7	7/7 (6)	–	NSA
10^5	8/8	8/8	8/8 (6)	–	NSA
10^4	8/8	8/8	8/8 (7)	–	NSA
10^3	5/8	4/8	4/8 (8·25)	–	0/4
10^2	1/8	1/8	1/8 (14)	0·403	1/8
HVP2ap					
10^6	5/8	0/8	0/8	0·382 (0·235–0·513)	8/8
10^5	1/8	0/8	0/8	0·321 (0·154–0·558)	8/8
10^4	1/8	0/8	0/8	0·436 (0·170–0·594)	6/8
10^3	0/8	0/8	0/8	–	0/8
10^2	0/8	0/8	0/8	–	0/8

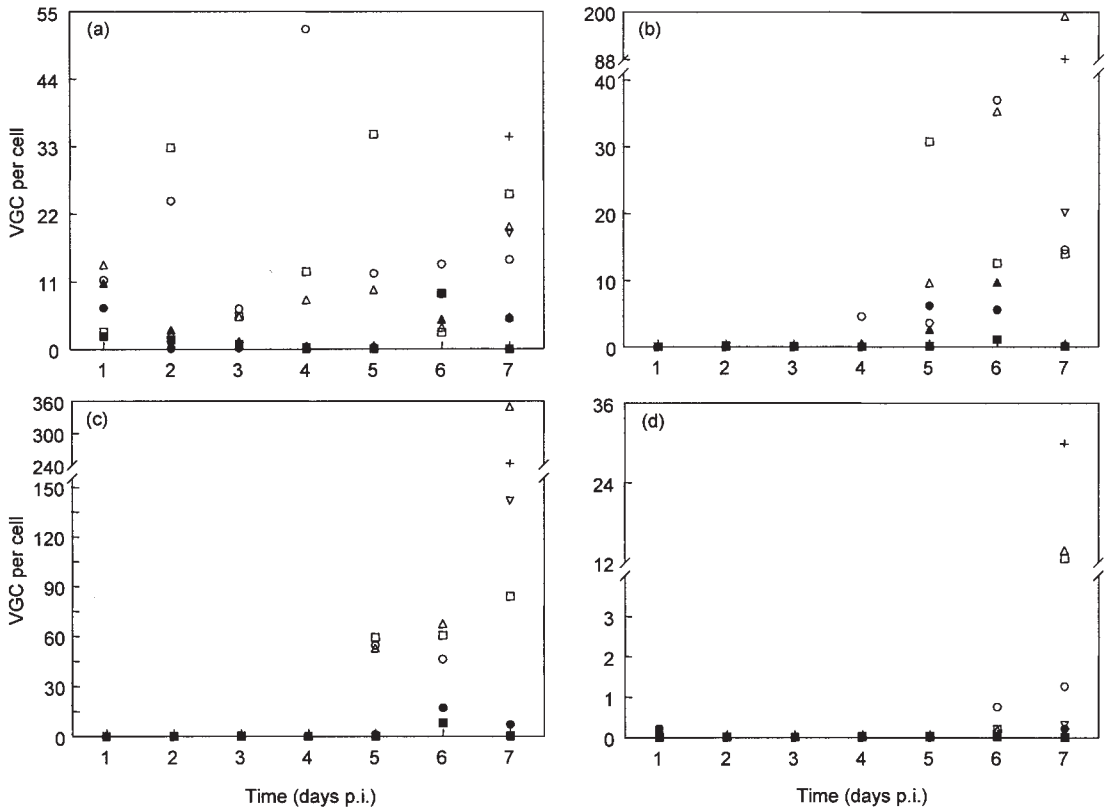

Fig. 3. Real-time PCR quantification of VGC per cell in HVP2-infected mouse tissues 1–7 days p.i. Filled symbols (■, ▲, ●) represent individual HVP2ap-infected mice and open symbols (□, △, ○, +, ▽) identify individual HVP2nv-infected mice. Tissues examined were skin from the site of inoculation (a), lumbar spinal cord (b), thoracic spinal cord (c) and brainstem (d).

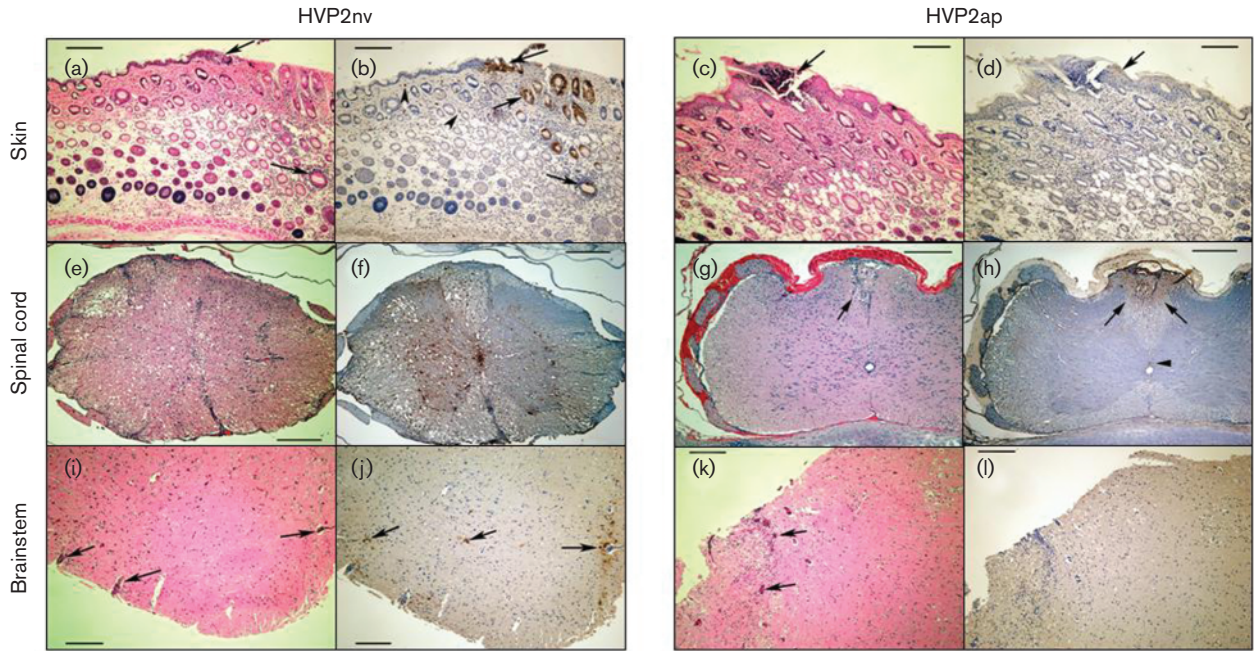

Fig. 4. Histological lesions present in mice infected with HVP2. (a–d) Skin. HVP2nv-infected mice exhibited a dermatitis with epidermal hyperplasia and necrosis of both epidermal and follicular epithelium (arrow; a). Viral antigen was conspicuous within epidermal and follicular epithelial cells (arrows; b). Non-specific staining labelled dermal mast cells (arrowheads, b). HVP2ap-infected mice showed focal effacement of the epidermis at the scarification site (arrow, c) with scant viral antigen predominantly in epidermal epithelial cells (arrow, d). (e–h) Spinal cord. HVP2nv-infected mice exhibited severe inflammation, spongiosis and necrosis in both ipsilateral and contralateral regions of the spinal cord (e) accompanied by widely distributed viral antigen by IHC (f). In HVP2ap-infected mice, lesions were restricted to mild mononuclear inflammation and subtle spongiosis of the ipsilateral dorsal funiculus (arrow, g). Viral antigen detected by IHC was predominantly seen in the lesional ipsilateral dorsal funiculus (arrows, h) with scant isolated staining near the central canal (arrowhead, h). (i–l) Brainstem. Lesions consisting primarily of perivascular cuffing (arrows; i, k) by mononuclear inflammatory cells were present in one mouse each (8 days p.i.) from the HVP2nv-infected (i) and HVP2ap-infected (k) mice. By IHC staining, viral antigen was distributed throughout the brainstem of HVP2nv-infected mice (arrows; j), but was not detectable in the brainstem of HVP2ap-infected mice (l). Sections were prepared by H&E stain (a, c, e, g, i, k) or by IHC with Mayer's haematoxylin counterstain (b, d, f, h, j, l). Bars, approx. 180 μm (a–d, i–l) and 250 μm (e–h).

At 5 days p.i., spinal cord lesions were similar between mice infected with the two HVP2 subtypes, being characterized by mild infiltrates of mononuclear cells within the ipsilateral dorsal funiculus and overlying meninges of the lumbar spinal cord. By day 7 p.i., HVP2nv-infected mice exhibited severe inflammation and spongiosis in all regions of the thoracic and lumbar spinal cord (Fig. 4e), while spinal cord lesions in HVP2ap-infected mice (Fig. 4g) were restricted to the ipsilateral dorsal funiculus of the lumbar and thoracic spinal cord and never developed to the level of severity observed in HVP2nv-infected mice. By IHC, viral antigen distribution correlated with histological lesions, the intensity of viral antigen staining being greater in HVP2nv-infected mice than in HVP2ap-infected animals (Fig. 4f, h).

Histopathological lesions within the brainstem were seen at 8 days p.i. in one animal each from the HVP2nv- and HVP2ap-infected groups. While the lesions were nearly identical in character (Fig. 4i, k), viral antigen was markedly conspicuous in the HVP2nv-infected mouse but scant in the HVP2ap-infected mouse (Fig. 4j, l).

HVP2 pathogenicity via i.c. inoculation

Inoculation of high doses of HVP2ap by s.s. resulted in a productive infection, despite a lack of clinical signs of CNS infection, evidenced by both seroconversion and CNS lesions. These data suggested two possible reasons for the apathogenicity of HVP2ap: (i) inefficient virus replication or control of the virus by the host innate immune system at the site of inoculation does not allow generation of sufficient virus for efficient CNS invasion or (ii) HVP2ap is deficient for replication within tissues of the CNS. To test this second possibility, groups of five mice were inoculated i.c. with doses of HVP2nv ranging from 10^0 to 10^6 p.f.u. or with 10^2–10^6 p.f.u. HVP2ap. The ID_{50} value for HVP2nv following i.c. inoculation was $<10^1$ p.f.u., while the two HVP2ap isolates had ID_{50} values of $10^{5\cdot1}$ (A951) and

Table 2. HVP2 pathogenesis in mice following i.c. inoculation

Values for death are the numbers of mice in each group that died or were humanely euthanized prior to 14 days p.i. The mean survival time for groups of mice following i.c. inoculation is given in days p.i. Numbers in parentheses represent the range of survival times for mice in each group; ND, no death. For the ELISA, absorbance shows the mean A_{490} for positive sera (positive cut-off $\geqslant 0{\cdot}100$) for anti-HVP2 IgG in serum from mice collected 7–19 days p.i. Numbers in parentheses are the range of A_{490} values of positive sera. Seropositivity shows the number of positive sera/total number of sera tested. Sera were not tested for mice that died prior to 7 days p.i.; NSA, no sera available for testing.

Dose (p.f.u.)	Death	Mean survival time (days p.i.)	ELISA	
			Absorbance	Seropositivity
HVP2nv				
10^6	4/4*	1·39 (1·0–2·0)	–	NSA
10^5	5/5	1·42 (1·27–2·0)	–	NSA
10^4	5/5	4·20 (4·0–5·0)	–	NSA
10^3	5/5	5·60 (5·0–7·0)	–	NSA
10^2	5/5	5·80 (5·0–6·0)	–	NSA
10^1	4/5	6·75 (6·0–7·0)	0·283 (0·228–0·340)	4/5
10^0	2/5	8·50 (6·0–11·0)	0·641 (0·151–1·130)	2/3†
HVP2ap OU2-5				
10^6	4/5	1·45 (1·27–2·0)	–	NSA
10^5	0/5	ND	0·142 (0·112–0·168)	4/5
10^4	0/5	ND	0·186 (0·140–0·231)	2/5
10^3	0/5	ND	–	0/5
10^2	0/5	ND	–	0/5
HVP2ap A951				
10^6	1/5	2·00	0·140	4/4
10^5	0/4	ND	0·113	1/4
10^4	0/5	ND	–	0/5
10^3	0/5	ND	–	0/5
10^2	0/5	ND	–	0/5

*One mouse survived to 7 days p.i. The large degree of variation from the group mean time of death suggested experimental error and the mouse was dropped from the experiment.
†Both mice that died were found dead in the morning; serum was available only from the three survivors.

$10^{4·3}$ p.f.u. (OU2-5) (Table 2). Clinical signs of disease following i.c. inoculation included circling, hyperaesthesia, photophobia and ataxia demonstrated by incoordination and tip-toe walking. All mice that developed clinical signs required euthanasia, so that the $CNSD_{50}$ and LD_{50} values for HVP2nv were approximately 1 p.f.u. In contrast, the HVP2ap isolates A951 and OU2-5 had $CNSD_{50}$ and LD_{50} values of $10^{6·1}$ p.f.u. and $10^{5·9}$ p.f.u., respectively.

Histopathological staining of brains from mice inoculated with HVP2ap revealed that lesions were restricted to a non-suppurative meningitis and subependymal accumulations of granular material that was positive for viral antigen by IHC (Fig. 5a, b). Apart from these focal deposits that were accompanied by microglia, there were no inflammatory lesions or distribution of viral antigen distant from the site of inoculation noted within the brain. In contrast, mice that received HVP2nv exhibited inflammation, neuronal necrosis and viral antigen within the cerebrum as well as regions distant from the inoculation site, including the cerebellum and brainstem (Fig. 5c, d).

HVP2 pathogenicity via e.s. inoculation

Mice were inoculated with HVP2 by eye splash to determine whether HVP2 could enter the CNS through neural circuits without injury to the eye (corneal scarification), similar to what is thought to have occurred in a case of human BV infection (Anonymous, 1998). By 3 days p.i., all mice inoculated with 10^6 p.f.u. and one mouse inoculated with 10^5 p.f.u. HVP2nv had pronounced swelling and redness of the conjunctiva in the infected eye. Between 8 and 11 days p.i., all mice infected with 10^6 p.f.u. and one mouse each from the HVP2nv 10^5 and 10^3 p.f.u. groups either died or required euthanasia due to signs of severe CNS disease. Clinical signs of CNS disease were similar to those observed for mice infected i.c. A single mouse inoculated with 10^5 p.f.u. HVP2ap developed conjunctivitis at 6 days p.i.

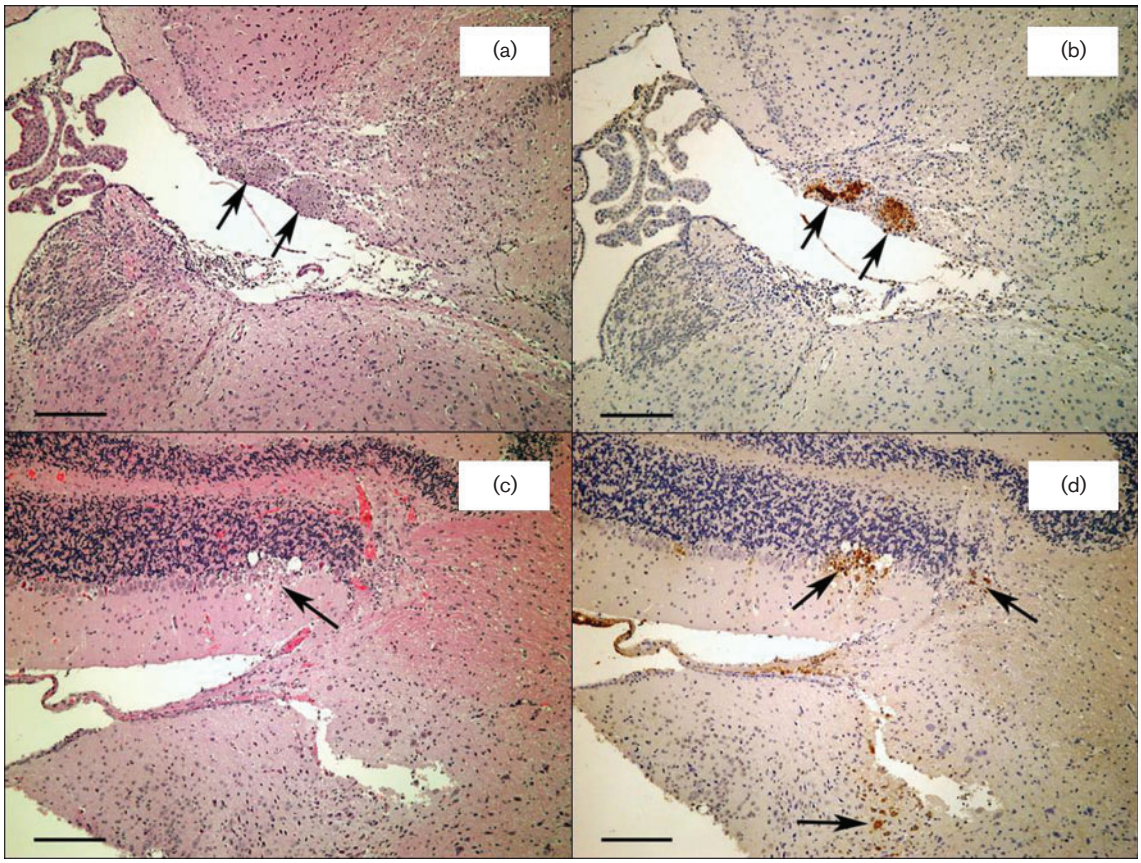

Fig. 5. Brain tissue from mice inoculated i.c. with HVP2. (a, b) Lesions in HVP2ap-infected mice included a mild to moderate non-suppurative meningitis and subependymal deposits of granular basophilic material (arrows; a) that were positive for viral antigen by IHC (arrows; b). (c, d) HVP2nv-infected mice exhibited evidence of dissemination of viral infection characterized by inflammation, necrosis and viral antigen distributed as far as the cerebellum and brainstem. In the cerebellum, the Purkinje cells were especially affected by necrosis (arrows; c) with confirmation of viral antigen by IHC (arrows; d). Sections were prepared by H&E stain (a, c) or by IHC stain with Mayer's haematoxylin counterstain (b, d). Bars, 180 μm.

similar to that observed in the HVP2nv-infected mice. However, the infection resolved by 10 days p.i. and the mouse remained healthy throughout the experiment.

DISCUSSION

While human BV infections are rare, the high rate of mortality associated with these infections is particularly startling. The availability of a safe, consistent and reproducible small animal model system amenable to molecular analysis and experimental studies would greatly facilitate elucidation of viral determinants responsible for the dichotomous behaviour of viruses in their natural versus aberrant host. HVP2nv produces infections in mice which closely parallel human BV infections in many ways and has the added benefit of being a safer, more convenient agent to work with experimentally. This study was undertaken to assess more fully the appropriateness of the HVP2/mouse system as an accurate model of zoonotic BV infections.

One alarming characteristic of human BV infections is that this virus readily invades the CNS regardless of the mode of inoculation. The first set of experiments was designed to evaluate the efficiency of HVP2 infection in mice using epidermal scarification to mimic what occurs during zoonotic transmission of BV via a scratch. For HVP2nv, skin lesions at the site of inoculation were significantly more severe following s.s compared with i.m., suggesting that HVP2nv replicates more efficiently in the skin than in muscle tissue. Although the LD_{50} value for HVP2nv was similar by s.s. and i.m. inoculation (Rogers *et al.*, 2003), all HVP2nv-infected mice inoculated with doses as high as 10^5 p.f.u. by s.s. were dead by 8 days p.i., while 2/8 mice inoculated i.m. with this same dose survived to 11 and 16 days p.i. and two additional mice survived to the termination of the experiment. Thus, inoculation of HVP2nv into the dermis results in more efficient invasion of the CNS and a more severe CNS infection. Weeks *et al.* (2000) showed that both HSV-1 and HSV-2 produced more severe primary and secondary lesions following flank scarification

compared with intradermal inoculation. Similarly, recent work with *Saimiriine herpesvirus 1* (a related α-herpesvirus of squirrel monkeys) demonstrated that more severe and consistent infections resulted in mice following epidermal inoculation compared with i.m. inoculation (Breshears *et al.*, 2005). Epidermal scarification permits efficient viral access to numerous free sensory nerve endings located above the basement membrane for ascension to neuronal cell bodies in the DRG. Once in the DRG, virus must again replicate and travel back down afferent neurons to the dermatome surrounding the site of inoculation to produce secondary lesions (zosteriform spread) and/or proceed cranially into the CNS. The temporal and spatial distribution of HVP2nv in the mouse CNS as well as the appearance of skin lesions at the site of inoculation that correlated with a rapid onset of CNS signs and death are both consistent with this scenario.

One interesting observation was the 'all-or-none' infection process in mice inoculated s.s. with HVP2nv: mice either developed a rapidly fatal CNS infection prior to the appearance of an HVP2-specific IgG response or they did not become infected as evidenced by a lack of seroconversion in surviving mice. The single exception was one mouse in the 10^2 p.f.u. dosage group that survived to 14 days p.i. and was seropositive at death. Experiments where virus was inoculated directly into the brain produced comparable results, indicating that once HVP2nv invades the nervous system the infection inexorably progresses to death. In contrast, both mice that survived i.m. inoculation with 10^5 p.f.u. HVP2nv displayed mild CNS signs which resolved over the course of the experiment, and others that survived at least 10 days p.i. were seropositive, even those that did not display clinical signs of CNS infection. Following i.m. inoculation, virus deposited into muscle tissue would be able to elicit an immune response, even if it was unable to gain entry into the CNS to cause overt disease. Since s.s. inoculation gives the virus direct access to free sensory nerve endings present in the dermis, it is easier for the virus to enter into these sensory nerves for transport to the DRG and entry into the CNS. If the virus is unable to gain entry into the nerves for some reason (e.g. low inoculum dose), the virus may be controlled by the innate immune system such that a specific immune response is not induced and no clinical disease develops. If in humans BV also either invades the nervous system, resulting in an extremely severe and generally fatal infection, or does not successfully enter the nervous system and is controlled by a local immune response, this could explain the lack of any concrete evidence of asymptomatic BV infections in humans (Freifeld *et al.*, 1995).

Although most human BV infections have been attributed to macaque bites or scratches, needle sticks or abrasive contact with contaminated fomites, there is a single reported case of a human infection resulting from contaminated fluid entering the CNS through an eye splash (Anonymous, 1998). The results of the HVP2 e.s. inoculation of mice demonstrate that, while HVP2nv replicates within the eye, only very high doses consistently produce a severe, fatal CNS infection. The relative inefficiency of HVP2nv entry into the CNS through an uninjured eye may reflect a similar situation in human BV infections, thus explaining the dearth of documented cases attributed to an eye splash. Further, while the eye splash is an ineffective route of entry for HVP2 into the CNS, the fact that only HVP2nv caused CNS disease further strengthens the conclusion that the pathogenic phenotypes of the two HVP2 subtypes are consistent regardless of route of inoculation.

One distinct asset of the HVP2nv/mouse system is the existence of HVP2ap isolates that provide a 'ready-to-use', naturally occurring apathogenic form of HVP2nv. The fact that the majority of HVP2 isolates characterized to date represent the HVP2nv subtype suggests that HVP2nv represents the wild-type while HVP2ap is a somewhat less successful mutant. As a first step in determining how HVP2nv and HVP2ap differ within the mouse model, the temporal progression of HVP2ap was compared with that of HVP2nv following s.s. inoculation of mice. Regardless of the peripheral replication of HVP2ap at the site of inoculation and its ability to invade the CNS, no clinical signs of CNS disease were noted in any HVP2ap-infected mice following s.s. infection with doses as high as 10^6 p.f.u. In addition, IHC staining of brain tissue samples from mice inoculated i.c. with HVP2ap revealed that HVP2ap was effectively sequestered at the site of inoculation, suggesting that HVP2ap is not competent for spread within the brain. These results suggest that a lack of neurovirulence and not a lack of neuroinvasiveness is a major reason for the differences observed between HVP2ap and HVP2nv in mice. This information will be useful in discerning which virus genes differ between the two HVP2 subtypes and may account for the dichotomous pathogenicity in mice.

In conclusion, HVP2nv appears to behave in mice very similarly to BV in humans. Irrespective of the route of inoculation, HVP2nv readily invades the CNS and produces a fulminant ascending encephalomyelitis which proves fatal once virus reaches the brainstem. This neuropathogenic behaviour is observed for all HVP2nv strains tested and thus appears to be an inherent property of the virus and not peculiar to a single isolate. The degree of genetic relatedness between HVP2 and BV and their biological similarities (pathogenicity in mice, resistance to anti-HSV drugs, *in vitro* replication, etc.) coupled with a preponderance of evidence demonstrating just how closely HVP2 infection in mice parallels human BV infections all support the appropriateness of the HVP2nv/mouse system as a model for investigating zoonotic BV infections.

ACKNOWLEDGEMENTS

The authors thank Drs Roger Panciera, Melanie Breshears and Jean d'Offay for valuable discussions and insight, Ms Amy Jacobs and Ms Cari Ritchey for expert technical assistance and Ms Monica Mattmuller and Ms Sandra Horton, College of Veterinary Medicine, North

Carolina State University, for assistance with immunohistochemical stains. This study was supported by PHS grants P40 RR12317 and R01 RR07849.

REFERENCES

Anonymous (1998). Fatal Cercopithecine herpesvirus 1 (B virus) infection following a mucocutaneous exposure and interim recommendations for worker protection. *MMWR Morb Mortal Wkly Rep* **47**, 1073–1076, 1083.

Breshears, M. A., Eberle, R. & Ritchey, J. W. (2001). Characterization of gross and histological lesions in Balb/C mice experimentally infected with *Herpesvirus saimiri 1* (HVS1). *J Comp Pathol* **125**, 25–33.

Breshears, M. A., Eberle, R. & Ritchey, J. W. (2005). Temporal progression of viral replication and gross and histological lesions in Balb/C mice inoculated epidermally with *Saimiriine herpesvirus 1* (SaHV-1). *J Comp Pathol* **133**, 103–113.

Davidson, W. L. & Hummeler, K. (1960). B virus infection in man. *Ann N Y Acad Sci* **85**, 970–979.

Eberle, R. & Hilliard, J. K. (1984). Replication of simian herpesvirus SA8 and identification of viral polypeptides in infected cells. *J Virol* **50**, 316–324.

Eberle, R., Black, D. H., Lipper, S. & Hilliard, J. K. (1995). *Herpesvirus papio 2*, an SA8-like α-herpesvirus of baboons. *Arch Virol* **140**, 529–545.

Eberle, R., Black, D. H., Blewett, E. L. & White, G. L. (1997). Prevalence of *Herpesvirus papio 2* in baboons and identification of immunogenic viral polypeptides. *Lab Anim Sci* **47**, 256–262.

Eberle, R., Black, D. H., Lehenbauer, T. W. & White, G. L. (1998). Shedding and transmission of baboon *Herpesvirus papio 2* (HVP2) in a breeding colony. *Lab Anim Sci* **48**, 23–28.

Freifeld, A. G., Hilliard, J., Southers, J., Murray, M., Savarese, B., Schmitt, J. M. & Straus, S. E. (1995). A controlled seroprevalence survey of primate handlers for evidence of asymptomatic herpes B virus infection. *J Infect Dis* **171**, 1031–1034.

Gaillard, C. & Strauss, F. (1990). Ethanol precipitation of DNA with linear polyacrylamide as carrier. *Nucleic Acids Res* **18**, 378.

Gosztonyi, G., Falke, D. & Ludwig, H. (1992). Axonal and transsynaptic (transneuronal) spread of herpesvirus simiae (B virus) in experimentally infected mice. *Histol Histopathol* **7**, 63–74.

Ohsawa, K., Lehenbauer, T. W. & Eberle, R. (1999). *Herpesvirus papio 2*: alternative antigen for use in monkey B virus diagnostic assays. *Lab Anim Sci* **49**, 605–616.

Ritchey, J. W., Ealey, K. A., Payton, M. E. & Eberle, R. (2002). Comparative pathology of infections with baboon and African green monkey alpha-herpesviruses in mice. *J Comp Pathol* **127**, 150–161.

Ritchey, J. W., Payton, M. E. & Eberle, R. (2005). Clinicopathological characterization of monkey B virus (*Cercopithecine herpesvirus 1*) infection in mice. *J Comp Pathol* **132**, 202–217.

Robertson, J. L. & Preisler, H. K. (1992). *Pesticide Bioassays with Arthropods*, 2nd edn. Boca Raton, FL: CRC Press.

Rogers, K. M., Ealey, K. A., Ritchey, J. W., Black, D. H. & Eberle, R. (2003). Pathogenicity of different baboon *Herpesvirus papio 2* isolates is characterized by either extreme neurovirulence or complete apathogenicity. *J Virol* **77**, 10731–10739.

Weeks, B. S., Ramchandran, R. S., Hopkins, J. J. & Friedman, H. M. (2000). Herpes simplex virus type-1 and -2 pathogenesis is restricted by the epidermal basement membrane. *Arch Virol* **145**, 385–396.

Weigler, B. J. (1992). Biology of B virus in macaque and human hosts: a review. *Clin Infect Dis* **14**, 555–567.

Whitley, R. J. & Hilliard, J. K. (2001). Cercopithecine herpesvirus (B virus). In *Fields Virology*, 4th edn, vol. 2, pp. 2835–2848. Edited by P. M. Howley & D. M. Knipe. Philadelphia: Lippincott Williams & Wilkins.